

1 Supporting information for:

2  
3 **Insight into acid-base nucleation experiments by comparison of**  
4 **the chemical composition of positive, negative and neutral**  
5 **clusters**

6  
7 Federico Bianchi<sup>†</sup>, Arnaud P. Praplan<sup>‡</sup>, Nina Sarnela<sup>‡</sup>, Josef Dommen<sup>†</sup>, Andreas Kürten<sup>§</sup>,  
8 Ismael K. Ortega<sup>\*</sup>, Siegfried Schobesberger<sup>‡</sup>, Heikki Junninen<sup>‡</sup>, Mario Simon<sup>§</sup>, Jasmin  
9 Tröstl<sup>†</sup>, Tuija Jokinen<sup>‡</sup>, Mikko Sipilä<sup>‡</sup>, Alexey Adamov<sup>‡</sup>, Antonio Amorim<sup>r</sup>, Joao Almeida<sup>‡</sup>,  
10 Martin Breitenlechner<sup>‡,γ</sup>, Jonathan Duplissy<sup>‡,‡,§</sup>, Sebastian Ehrhart<sup>‡</sup>, Richard C. Flagan<sup>‡</sup>,  
11 Alessandro Franchin<sup>‡</sup>, Jani Hakala<sup>‡</sup>, Armin Hansel<sup>‡,γ</sup>, Martin Heinritzi<sup>‡,δ</sup>, Juha  
12 Kangasluoma<sup>‡</sup>, Helmi Keskinen<sup>‡</sup>, Jaeseok Kim<sup>‡</sup>, Jasper Kirkby<sup>‡,‡</sup>, Ari Laaksonen<sup>‡,‡</sup>, Michael  
13 J. Lawler<sup>‡,‡</sup>, Katrianne Lehtipalo<sup>‡,‡</sup>, Markus Leiminger<sup>‡</sup>, Vladimir Makhmutov<sup>‡</sup>, Serge  
14 Mathot<sup>‡</sup>, Antti Onnela<sup>‡</sup>, Tuukka Petäjä<sup>‡</sup>, Francesco Riccobono<sup>‡</sup>, Matti P. Rissanen<sup>‡</sup>, Linda  
15 Rondo<sup>‡</sup>, António Tomé<sup>r</sup>, Annele Virtanen<sup>‡</sup>, Yrjö Viisanen<sup>‡</sup>, Christina Williamson<sup>‡</sup>, Daniela  
16 Wimmer<sup>‡,‡</sup>, Paul M. Winkler<sup>‡</sup>, Penglin Ye<sup>‡</sup>, Joachim Curtius<sup>‡</sup>, Markku Kulmala<sup>‡</sup>, Douglas R.  
17 Worsnop<sup>‡,‡</sup>, Neil M. Donahue<sup>‡</sup>, and Urs Baltensperger<sup>†\*</sup>

18  
19 <sup>†</sup> Laboratory of Atmospheric Chemistry, Paul Scherrer Institute, Villigen 5232, Switzerland

20 <sup>‡</sup> Department of Physics, University of Helsinki, Helsinki 00014, Finland

21 <sup>§</sup> Institute for Atmospheric and Environmental Sciences, Goethe University Frankfurt am Main,  
22 Frankfurt am Main 60438, Germany

23 <sup>\*</sup> Laboratoire de Physique des Lasers, Atomes et Molécules, Université Lille 1 Sciences et  
24 Technologies, Villeneuve d'Ascq cedex 59655, France

25 <sup>r</sup> CENTRA-SIM, U. Lisboa and U. Beira Interior, Lisbon 1749, Portugal

26 <sup>‡</sup> CERN, Geneva 1211, Switzerland

27 <sup>δ</sup> University of Innsbruck, Innsbruck 6020, Austria

28 <sup>γ</sup> IONICON Analytik GmbH, Innsbruck 6020, Austria

29 <sup>§</sup> Helsinki Institute of Physics, Helsinki 00014, Finland

30 <sup>‡</sup> California Institute of Technology, California, Pasadena 91125, United States

31 <sup>†</sup> Department of Applied Physics, University of Eastern Finland, Kuopio 70211, Finland

32 <sup>‡</sup> Atmospheric Chemistry Division, National Center for Atmospheric Research, Colorado, Boulder  
33 80301, United States

34 <sup>‡</sup> Airmodus Ltd, Helsinki 00560, Finland

35 <sup>‡</sup> Lebedev Physical Institute RAS, Leninsky prospekt, Moscow 119991, Russian

36 <sup>‡</sup> Finnish Meteorological Institute, Helsinki 00101, Finland

37 <sup>‡</sup> Faculty of Physics, University of Vienna, Vienna 1090, Austria

38 <sup>‡</sup> Center for Atmospheric Particle Studies, Carnegie Mellon University, Pennsylvania, Pittsburgh  
39 15213, United States

40 <sup>‡</sup> Aerodyne Research Inc., Massachusetts, Billerica 01821, United States

41  
42 The supporting information contains 2 figures and 1 scheme on 9 pages.

43

#### 44 **The CLOUD chamber**

45 The CLOUD chamber is a 3m-diameter stainless-steel cylinder of 26.1 m<sup>3</sup> volume.  
46 Pure air, free of condensable vapors, is obtained from the evaporation of cryogenic  
47 liquid nitrogen and liquid oxygen mixed at a ratio of 79:21. Water vapor is added  
48 from an ultrapure source to a controlled relative humidity. The chamber can be  
49 irradiated by UV light (250-400 nm) to create hydroxyl (OH) radicals by photolysis of  
50 ozone in the presence of water vapor.<sup>41</sup> The chamber can be exposed to a 3.5 GeV/c  
51 secondary pion beam from the CERN Proton Synchrotron, spanning the galactic  
52 cosmic ray intensity range from ground level to the stratosphere. Activating an  
53 electric field of 20 kV/m in the chamber sweeps away all the ions produced by cosmic  
54 rays, on request, and allows to perform experiments also under neutral conditions.

55 To avoid contamination from plastic materials (especially organic compounds), all  
56 gas pipes are made from stainless steel, and most gas and chamber seals are gold  
57 coated. Despite all these measures traces of contaminants, e.g. small volatile organic  
58 compounds (VOCs)<sup>42</sup> and NH<sub>3</sub><sup>43</sup>, can still be observed. Even though dimethylamine  
59 (DMA) was initially absent in the thoroughly cleaned chamber (heated to 373 K),  
60 traces of DMA were detected once it had been injected, until the next thorough  
61 cleaning was performed (see discussion in the main text).<sup>23</sup>

62 The nucleation rates ( $J_{1.7}$ , cm<sup>-3</sup> s<sup>-1</sup>) were measured under neutral ( $J_n$ ), galactic  
63 cosmic rays ( $J_{gcr}$ ) and pion beam ( $J_\pi$ ) conditions, corresponding to ion-pair  
64 concentrations of about 0, 400 and 3000 ion pairs cm<sup>-3</sup>, respectively.

#### 65 **APi-TOF and CI-APi-TOF**

66 The chemical composition of the ions was studied using the Atmospheric Pressure  
67 interface Time-of-Flight mass spectrometer (APi-TOF).<sup>18,19,30</sup> The instrument is  
68 divided in two parts. The first part is the atmospheric pressure interface that  
69 efficiently guides ions into the mass spectrometer. It consists of two quadrupoles and  
70 an ion lens system. It is equipped with a critical orifice that provides a sample flow of  
71 0.8 l min<sup>-1</sup>. The second part is the high transmission efficiency time-of-flight mass  
72 spectrometer that allows retrieval of mass-to-charge ratio of charged clusters smaller  
73 than ~2 nm diameter.

74 The APi-TOF mass spectrometers, manufactured by ToFwerk AG (Thun,  
75 Switzerland) and Aerodyne Research, Inc. (Billerica, MA, USA), have a resolving  
76 power close to 5000 (full width at half maximum FWHM at  $m/z > 200$ ) and a mass

77 accuracy better than 10 ppm. The data were analyzed using a Matlab based set of  
78 programs (tofTools) developed at the University of Helsinki.<sup>18</sup> When the APi-TOF is  
79 not coupled to an ion source, it measures the composition of airborne charged  
80 clusters. In the CLOUD chamber, ions are formed by galactic cosmic rays (GCR) or  
81 by the pion beam from the Proton Synchrotron. Varying the intensity of the beam thus  
82 changes the ion concentration inside the chamber. We can regard the combination of  
83 the CLOUD chamber and the APi-TOF as an oversized Chemical Ionization Mass  
84 Spectrometer (CIMS) where the CLOUD chamber acts as ion source. However it  
85 should be noted here that an important difference between the CLOUD chamber and a  
86 CIMS ion source is the extremely long ion reaction time and the poorly defined ion  
87 distribution in the chamber. During the experiments described here, two APi-TOF  
88 were operated in parallel: the first one in negative mode (APi-TOF(-)) and the other  
89 one in positive mode (APi-TOF(+)). This allowed the simultaneous characterization  
90 of the negative and positive ions during the nucleation experiments.

91 In CLOUD the primary positive and negative ions produced in the chamber are  
92 mainly  $\text{N}_2^+$ ,  $\text{O}_2^+$ ,  $\text{N}^+$  and  $\text{O}^+$ , and  $\text{O}^-$  and  $\text{O}_2^-$ , respectively.<sup>44</sup> These ions undergo rapid  
93 ion-molecule reactions; the positive ions react quickly with water vapor to form  
94 protonated water clusters.<sup>44</sup> Then the charge is transferred to trace bases such as  
95 ammonia and amines that are present in the chamber as impurities. On a similar time  
96 scale, the small negative ions react quickly with nitric acid ( $\text{HNO}_3$ ) and  $\text{H}_2\text{SO}_4$  to  
97 form ions such as  $(\text{H}_2\text{O})_n(\text{acid})_m\text{NO}_3^-$  (where acid represents  $\text{HNO}_3$  and/or  $\text{H}_2\text{SO}_4$ ).<sup>22</sup>  
98 The negative ions are dominated by compounds with a high gas-phase acidity,  
99 whereas in the positive case the main ions are formed from compounds with a high  
100 proton affinity. For example, under clean conditions (beginning of the campaign)  
101 pyridinium ( $\text{C}_5\text{H}_6\text{N}^+$ ) was typically found as the main positive ion and nitrate ( $\text{NO}_3^-$ )  
102 as the negative ion.

103 Charged clusters can be formed by two different mechanisms. Either a precursor of  
104 the cluster is ionized and forms stable clusters after collision with other compounds  
105 present in the gas phase (ion-induced nucleation, IIN)<sup>45, 46</sup> or a neutral cluster receives  
106 a charge by diffusion charging. In the latter case the charge is transferred from  
107 another compound to the cluster after its (neutral) formation, e.g. by a proton transfer  
108 reaction or by clustering with an ion.

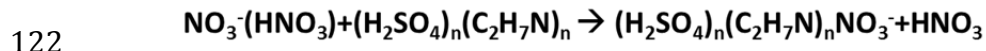
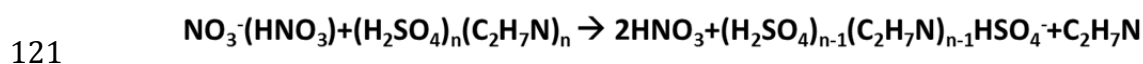
109 As already mentioned, the chemical composition of the ions was determined only  
110 for GCR and pion beam conditions, since the APi-TOF can only measure charged

111 clusters. However, recently, the APi-TOF was augmented by adding a chemical  
112 ionization source in front of it.<sup>21,47</sup> This instrument is called Chemical Ionization APi-  
113 TOF (CI-APi-TOF) mass spectrometer. It is able to detect neutral clusters after  
114 ionization by a chemical reaction.

115 The reagent ions used in this study for chemical ionization are  $\text{NO}_3^-(\text{HNO}_3)_{0-2}$ .<sup>48</sup>  
116 The ionization proceeds either via a proton transfer reaction (i.e., de-protonation of  
117  $\text{H}_2\text{SO}_4$  to  $\text{HSO}_4^-$ ) or by cluster formation between the neutral compounds and the  
118 nitrate ions (Scheme S1):

119

120 **Scheme S1.** Reaction between the primary ion and the clusters in the CI unit.

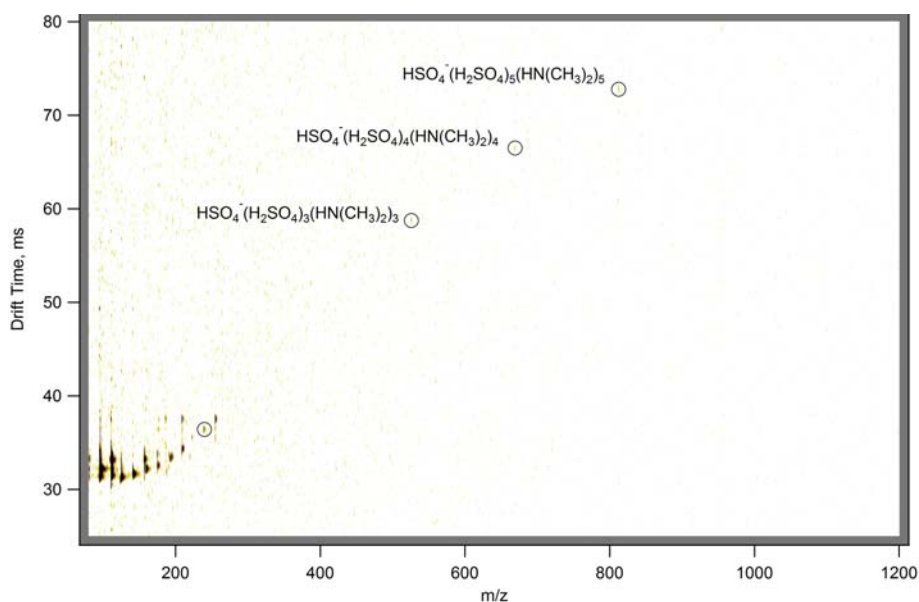


123 With this method, it was possible to identify for the first time in CLOUD the neutral  
124 clusters that were participating in the nucleation process.

125 It is important to note that the chemical composition of the clusters can change  
126 when they enter the APi-TOF or even before when they get ionized in the CI-region.  
127 At the moment, evaporation and fragmentation of clusters inside the APi-TOF mass  
128 spectrometer is not well characterized. For example, it is well known that clusters  
129 contain water in the atmosphere, however all the clusters that have been identified in  
130 these experiments do not. Water binds only weakly to the clusters in most cases, with  
131 evaporation rates of  $10^5$ - $10^6$   $\text{s}^{-1}$ .<sup>16</sup> Thus, the only reason to have it in clusters is the  
132 high collision frequency of water with the cluster due to the extremely high  
133 concentration of water in the atmosphere. When the cluster enters the APi-TOF the  
134 collision rate with water drops substantially and the water is lost from the clusters.  
135 Evaporation of sulfuric acid or bases might also occur as was inferred from a  
136 comparison of measured and modeled molecular cluster distributions.<sup>32</sup> For more  
137 details see the supplement information of Almeida et al. (2013) [ref. 16].

138 As already mentioned, under the condition of no collisional heating in the MS-inlet  
139 we expect water to evaporate but not the base molecules. However, if there is enough  
140 collisional heating, this may also happen and there is evidence that this happens for  
141 small clusters as observed from some measurements with the ion-mobility-

142 spectrometer-TOF-MS (IMS-TOF). However, our data base is still too small to draw  
143 firm conclusions and therefore these results will be subject of future papers.



144

145 **Figure S1.** 2D plot of drift time vs mass-to-charge ratio of sulfuric acid-DMA  
146 clusters measured during the run 1047.01 with the IMS-TOF. The negative clusters  
147 containing 3, 4 and 5 molecules of sulfuric acid are the ones with the best signal-to-  
148 noise ratio in both dimensions. Sulfuric acid-DMA clusters are highlighted by open  
149 black circles.  
150

151 Results as presented in Figure S1 show the drift time and their mass spectrum of the  
152 clusters that are present in the CLOUD chamber during a nucleation experiment  
153 involving sulfuric acid and DMA (Run 1047.01). The strongest signals arise from  
154 small ions (black dots bottom left). These ions show that there are a lot of compounds  
155 with the same drift time but different mass, indicative of fragmentation inside the  
156 API-TOF. However this plot also shows that bigger clusters are less prone to  
157 fragmentation since there are no other smaller clusters with the same drift time.

158 Quantum chemical calculations show that the clusters with an excess of sulfuric  
159 acid or bases (>2) are much less stable than the clusters we observed here mostly.  
160 Therefore, it is likely that these cases do not need to be considered as important.

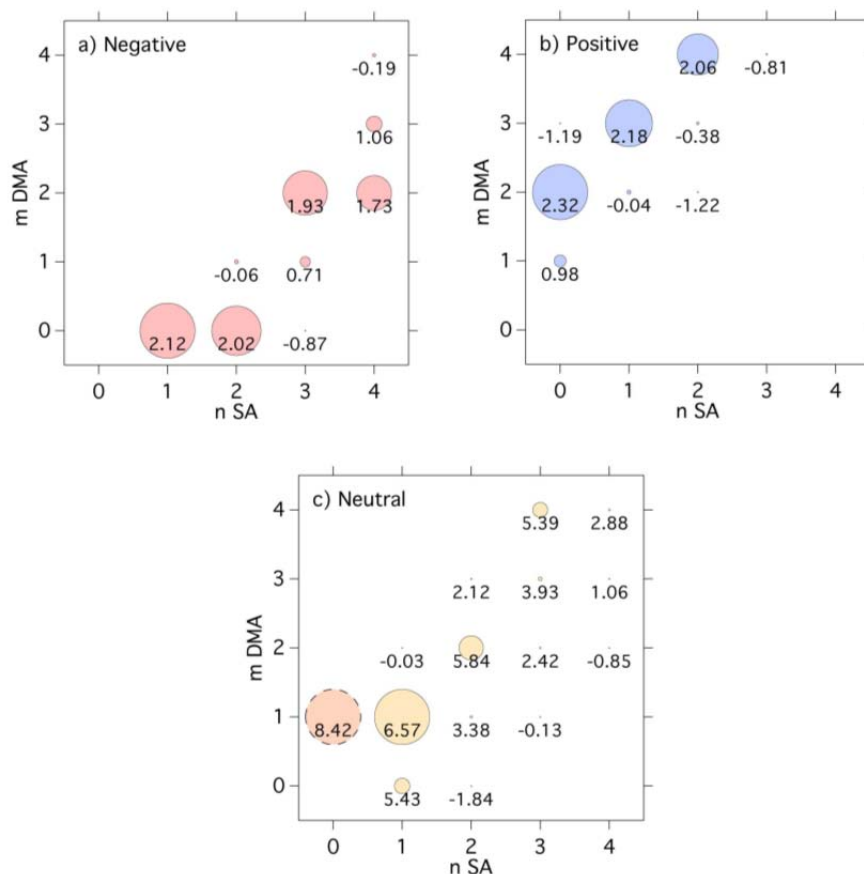
161

162 When we compare the cluster time evolution the three different mass spectrometers  
163 do not consider water. These instruments have the same identical issue regarding the  
164 impossibility of measuring water in the clusters. However for the purpose of this  
165 comparison it is not crucial to see the water molecules in the clusters.

166

167 The second source of possible cluster fragmentation could be in the chemical  
168 ionization unit. This kind of fragmentation has already been observed during CLOUD  
169 experiments and it was discussed in a previous study.<sup>16</sup> The main reason of this  
170 fragmentation is that the stabilization of the clusters occurs via proton-transfers or –  
171 hydrogen bridges, and ionization adds/removes one of those. Quantum chemical  
172 calculations show that the clusters will always loose bases when they get charged  
173 negatively and they will loose sulfuric acid when they are charged positively.<sup>31</sup> As the  
174 clustering process is driven by acid base chemistry, the key is that for neutral clusters  
175 the optimum acid:base ratio is different to the one for positive or negative clusters  
176 (mainly because ions are acids or bases and there is some competition with sulfuric  
177 acid or ammonia/DMA). Just note that sulfuric acid, once it is deprotonated is a base  
178 and therefore if the cluster is small the DMA in excess will “leave” the cluster.

179 Excluding evaporation inside the mass spectrometer, the APiTOF measures the  
180 composition of the ions as they occur in the atmosphere or in the CLOUD chamber.  
181 Therefore, this loss of acids or bases due to ionization is not a measurement artifact,  
182 but the representation of what happens in the atmosphere when the ions are formed. It  
183 is an issue for the measurements of the neutral clusters by CI-APiTOF. Here,  
184 chemical ionization of the neutral clusters may change the composition. This is  
185 certainly true for small clusters while it is expected to be less severe for larger  
186 clusters. Moreover, the neutral clusters will have a certain acid:base ratio and clusters  
187 with an excess of base or acid will not be stable, only clusters with the optimum  
188 acid:base ratio and maybe +/- 2 acids or bases will be stable and persist much longer.  
189 Looking at quantum chemical results published in Almeida et al. (2013) extended data  
190 Figure 4 (reproduced as Fig. S2 below) [ref 16], the clusters with the highest  
191 concentration fall more or less into the diagonal. For example in the case of clusters  
192 with one DMA molecule only those with 1 and 2 sulfuric acid molecules have  
193 significant concentrations, the concentration of clusters with 3 SA is rather low, and  
194 the one with 4 SA clusters is below  $0.01 \text{ cm}^{-3}$ . So there is no need to consider the loss  
195 of more than 1-2 SA or ammonia/DMA "excess" molecules, because the clusters with  
196 more than that will not be stable and probably will have very short lifetimes and their  
197 concentration will be extremely low if they are formed at all.



198

199 **Figure S2.** Theoretical concentrations of negative, positive and neutral clusters  
 200 during DMA ternary nucleation. Modelled steady-state concentrations (*mDMA* versus  
 201 *nSA*) at  $4.0 \times 10^6 \text{ cm}^{-3}$   $[\text{H}_2\text{SO}_4]$ , 10 pptv DMA, 4 ion pairs  $\text{cm}^{-3} \text{ s}^{-1}$  and 278 K. **a**,  
 202 negative clusters. **b**, positive clusters. **c**, neutral clusters. A sticking probability of 0.5  
 203 is assumed for all neutral–neutral collisions and 1.0 for all charged–neutral  
 204 collisions. The numbers below the center of each circle show  $\log_{10}C$ , where  $C$  ( $\text{cm}^{-3}$ )  
 205 is the cluster concentration (the threshold is  $0.01 \text{ cm}^{-3}$ ). The circle areas within each  
 206 panel are proportional to  $C$  (with the exception of the DMA monomer in **c**).  
 207 (Reproduced from Almeida et al., Nature, 2013)<sup>16</sup>

208

209 Moreover, Fig. S2 also shows that the most favorable acid:base ratios are different  
 210 for neutral, positive and negative clusters. The most abundant neutral clusters fall in  
 211 the diagonal, the negative clusters are below the diagonal (less bases) and the positive  
 212 ones above the diagonal (less acids).

213

214 REFERENCES:

215 41. Kupc, A.; Amorim, A.; Curtius, J.; Danielczok, A.; Duplissy, J.; Ehrhart, S.;  
 216 Walther, H.; Ickes, L.; Kirkby, J.; Kurten, A.; Lima, J. M.; Mathot, S.; Minginette, P.;  
 217 Onnela, A.; Rondo, L.; Wagner, P. E., A fibre-optic UV system for H(2)SO(4)  
 218 production in aerosol chambers causing minimal thermal effects. *J. Aerosol. Sci.*  
 219 **2011**, 42, (8), 532-543.

220 42. Schnitzhofer, R.; Metzger, A.; Breitenlechner, M.; Jud, W.; Heinritzi, M.; De  
221 Menezes, L. P.; Duplissy, J.; Guida, R.; Haider, S.; Kirkby, J.; Mathot, S.; Minginette,  
222 P.; Onnela, A.; Walther, H.; Wasem, A.; Hansel, A.; the, C. T., Characterisation of  
223 organic contaminants in the CLOUD chamber at CERN. *Atmos. Meas. Tech.* **2014**, *7*,  
224 (7), 2159-2168.

225 43. Bianchi, F.; Dommen, J.; Mathot, S.; Baltensperger, U., On-line determination  
226 of ammonia at low pptv mixing ratios in the CLOUD chamber. *Atmos. Meas. Tech.*  
227 **2012**, *5*, (7), 1719-1725.

228 44. Smith, D.; Spanel, P., Ions in the terrestrial atmosphere and in interstellar  
229 clouds. *Mass Spectrom. Rev.* **1995**, *14*, (4-5), 255-278.

230 45. Fangqun, Y.; Turco, R. P., Ultrafine aerosol formation via ion-mediated  
231 nucleation. *Geophys. Res. Lett.* **2000**, *27*, (6), 883-886.

232 46. Lee, S. H.; Reeves, J. M.; Wilson, J. C.; Hunton, D. E.; Viggiano, A. A.;  
233 Miller, T. M.; Ballenthin, J. O.; Lait, L. R., Particle formation by ion nucleation in the  
234 upper troposphere and lower stratosphere. *Science* **2003**, *301*, (5641), 1886-1889.

235 47. Jokinen, T.; Sipila, M.; Junninen, H.; Ehn, M.; Lonn, G.; Hakala, J.; Petaja, T.;  
236 Mauldin, R. L.; Kulmala, M.; Worsnop, D. R., Atmospheric sulphuric acid and  
237 neutral cluster measurements using CI-API-TOF. *Atmos. Chem. Phys.* **2012**, *12*, (9),  
238 4117-4125.

239 48. Viggiano, A. A.; Seeley, J. V.; Mundis, P. L.; Williamson, J. S.; Morris, R. A.,  
240 Rate constants for the reactions of  $XO_3-(H_2O)(n)$  ( $X = C, HC, \text{ and } N$ ) and  $NO_3-$   
241  $(HNO_3)(n)$  with  $H_2SO_4$ : Implications for atmospheric detection of  $H_2SO_4$ . *Journal*  
242 *of Physical Chemistry A* **1997**, *101*, (44), 8275-8278.

243